LETTERS

The Role of Vegetation–Climate Interaction and Interannual Variability in Shaping the African Savanna

NING ZENG AND J. DAVID NEELIN

Department of Atmospheric Sciences and Institute of Geophysics and Planetary Physics, University of California, Los Angeles, Los Angeles, California

29 November 1999 and 20 February 2000

ABSTRACT

Using a coupled atmosphere–land–vegetation model of intermediate complexity, the authors explore how vegetation–climate interaction and internal climate variability might influence the vegetation distribution in Africa. When the model is forced by observed climatological sea surface temperature (SST), positive feedbacks from vegetation changes tend to increase the spatial gradient between desert regions and forest regions at the expense of savanna regions. When interannual variation of SST is included, the climate variability tends to reduce rainfall and vegetation in the wetter regions and to increase them in the drier regions along this gradient, resulting in a smoother desert–forest transition. This effect is most dramatically demonstrated in a model parameter regime for which multiple equilibria (either a desertlike or a forestlike Sahel) can exist when strong vegetation–climate feedbacks are allowed. However, the presence of a variable SST drives the desertlike state and the forestlike state toward an intermediate grasslike state, because of nonlinearities in the coupled system. Both vegetation and interannual variability thus play active roles in shaping the subtropical savanna ecosystem.

1. Introduction

Although the world's vegetation distribution is determined largely by climate (Woodward 1987), the alteration of land and vegetation surface can, in turn, influence the climate. Examples include deforestation experiments for the Amazon (Dickinson and Henderson-Sellers 1988; Lean and Warrilow 1989; Shukla et al. 1990; Sud et al. 1996; Zhang et al. 1996), desertification experiments for the Sahel (Charney 1975; Xue and Shukla 1993), and experiments with the boreal forest (Bonan et al. 1992). Recent modeling is beginning to address the two-way interaction of vegetation and climate (Henderson-Sellers 1993; Claussen 1994; Ji 1995; Dickinson et al. 1998; Foley et al. 1998; Ganopolski et al. 1998).

Claussen (1994, 1998) and Claussen et al. (1998) coupled the ''BIOME'' equilibrium vegetation model (Prentice et al. 1992) to the European Centre for Medium-Range Forecasts–Deutsches Klimarechenzentrum: Hamburg (ECHAM) GCM in an asynchronous fashion and found that multiple equilibrium vegetation–climate states can exist in the present-day semidesert regions of northern Africa and western Asia. Wang and Eltahir (2000) studied the stability of similar states in response to disturbances. Brovkin et al. (1998) use a conceptual model to compare desert versus ''green'' equilibria under parameter estimates typical of current climate and of mid-Holocene climate, respectively.

A rarely considered factor in these studies is natural climate variability. As one of the most climatically sensitive and ecologically unstable regions in the world, the Sahel exhibits strong variability in both precipitation and vegetation on interannual and longer timescales (Goward and Prince 1995; Nicholson et al. 1998). The range of interannual and interdecadal rainfall variation can be as large as 50% of the climatological value (Zeng et al. 1999). The very existence of the savanna ecosystem is closely related to environmental variability in a non-equilibrium fashion (Ellis and Swift 1988).

Here a coupled tropical atmosphere–land–vegetation model of intermediate complexity is employed to address vegetation–climate interaction in the African savanna regions; in particular, the consequences of this interaction for the formation and maintenance of the savanna ecosystem in the presence of interannual and interdecadal climate variability that arises from other components of the climate system such as the oceans is addressed.

2. Models

The atmospheric component of the coupled model is the Quasi-Equilibrium Tropical Circulation Model

Corresponding author address: Ning Zeng, Department of Atmospheric Sciences, UCLA, Los Angeles, CA 90095-1565.
E-mail: zeng@atmos.ucla.edu

(QTCM), (Neelin and Zeng 2000, Zeng et al. 2000, hereinafter referred to as ZNC). This component is coupled to the land surface model known as Simple Land (SLand, ZNC), which represents the first-order effects relevant to climate simulation. In particular, the evapotranspiration is controlled by a stomatal-resistance. In the original version of SLand, the canopy resistance depends only on soil moisture. The current version takes into account the effects of leaf-to-canopy scaling following the method of Sellers et al (1996), such that the canopy conductance for evapotranspiration is

$$g_c = g_{s_{\max}} \beta(w)[1 - \exp(-kL)]/k, \quad (1)$$

where $g_{s_{\max}}$ is a maximum conductance, β depends on soil moisture w as used in the original SLand, L is the plant leaf area index, and k is the extinction coefficient of sunlight. Besides modifying evapotranspiration through (1), vegetation also changes land surface albedo A as

$$A = 0.38 - 0.25V. \quad (2)$$

This equation corresponds to an albedo of 0.38 at $V = 0$ (sandy desert), and 0.13 at $V = 1$ (dense forest), where V is vegetation fraction (normalized between 0 and 1). Thus, in the model, vegetation feeds back into the atmosphere by modifying surface energy and water fluxes through (1) and (2).

Vegetation is simulated following a simple formula describing biomass change:

$$\frac{dV}{dt} = \left(\frac{P^a}{P^a + P_0^a} - V \right) \Big/ \tau, \quad (3)$$

where P is precipitation, P_0 and a are parameters to be specified, and τ is the vegetation growth or loss timescale. This formula is similar to other empirically based models (Lieth 1975; Brovkin et al. 1998), also resembles the biomass equations used in models with explicit vegetation dynamics (Ji 1995; Foley et al. 1996; Dickinson et al. 1998), and has both a precipitation-dependent growth term and a loss term. The main features of the equilibrium solution (dV/dt set to zero) are that as P increases from zero V increases slowly but accelerates near an inflection point at P_0 ($P_0 = 900$ mm yr^{-1}) and gets saturated toward 1 as P becomes very large. Plant competition is not modeled explicitly, nor are species-specific characteristics considered; V is interpreted as a potential vegetation amount or leaf biomass. The vegetation is normalized between 0 and 1 and L is assumed to be proportional to V with $L = L_{\max}V$, where $L_{\max}$ is a maximum L taken as 8. The vegetation timescale is set at 24 yr, approximating plant succession such as the transition from grassland to forest. The model is run at a 5.625° long by 3.75° lat resolution. Over the ocean, SST is prescribed, either as the observed seasonal cycle of climatological SST or with interannual SST variability included. Whereas the atmosphere and land components use a time step of 20 min, the vegetation component [(3)] is run at a time step of 1 yr forced by annual mean precipitation from the atmospheric model.

3. Results

A series of experiments with the coupled atmosphere–vegetation model forced by climatological SST was conducted first. Vegetation is interactive only over Africa; QTCM–SLand's original surface types and associated surface albedo are used over the rest of the land regions. In these experiments, a is 64, which leads to a strong vegetation response to precipitation change around P_0. Figure 1a–c shows a pair of experiments that differ only in the initial vegetation distribution over the whole African continent, with the first experiment starting from a total desert (initial $V = 0$; ''DESERT''), and the second experiment starting from a fully forested Africa (initial $V = 1$; ''FOREST''). To ensure that the coupled model has reached equilibrium, the model was run for 250 yr. The equilibrium vegetation distribution is shown in Fig. 1. The final state of the DESERT run (Fig. 1a) shows a forested central Africa (V close to 1), extending to about 13°N and 13°S, and little vegetation poleward. For the FOREST run (Fig. 1b), the forested region extends about 400 km farther north to about 17°N and 17°S. The difference (FOREST − DESERT) in Fig. 1c shows two bands centered around 15°N and 15°S with a tendency to widen in some regions. These bands coincide approximately with the regions dominated by savanna in observations.

The existence of multiple equilibria corresponds to a regime suggested by Claussen et al. (1998), obtained with asynchronous coupling of an atmospheric general circulation model and an equilibrium vegetation model. In the model system presented here, many such pairs of experiments have been conducted to address uncertainties in the vegetation model parameters. The model also has been run at twice the horizontal resolution and returns qualitatively similar results. These sensitivity experiments show that the existence of multiple states depends on the parameter values in the vegetation–precipitation relation [(3)] and the evapotranspiration–vegetation relation [(1)]. The multiple equilibria exist in a range of parameters (a larger than 24) that we consider to be on the margin of the realistic estimates. A case for a more realistic parameter value of $a = 4$ is discussed below. In either case, it is found that a hitherto-unexplored factor has an overriding effect in smoothing out the vegetation gradient: interannual climate variability. Because this model permits many multicentury, synchronously coupled runs to be performed, we can address how variability affects the vegetation distribution in these climatically sensitive zones.

Precipitation in the Sahel is known to undergo strong interannual and interdecadal variation, largely in response to SST (Folland et al. 1986). Strictly speaking, vegetation should be considered to be part of the climate system on all timescales. Because the SST variability is caused

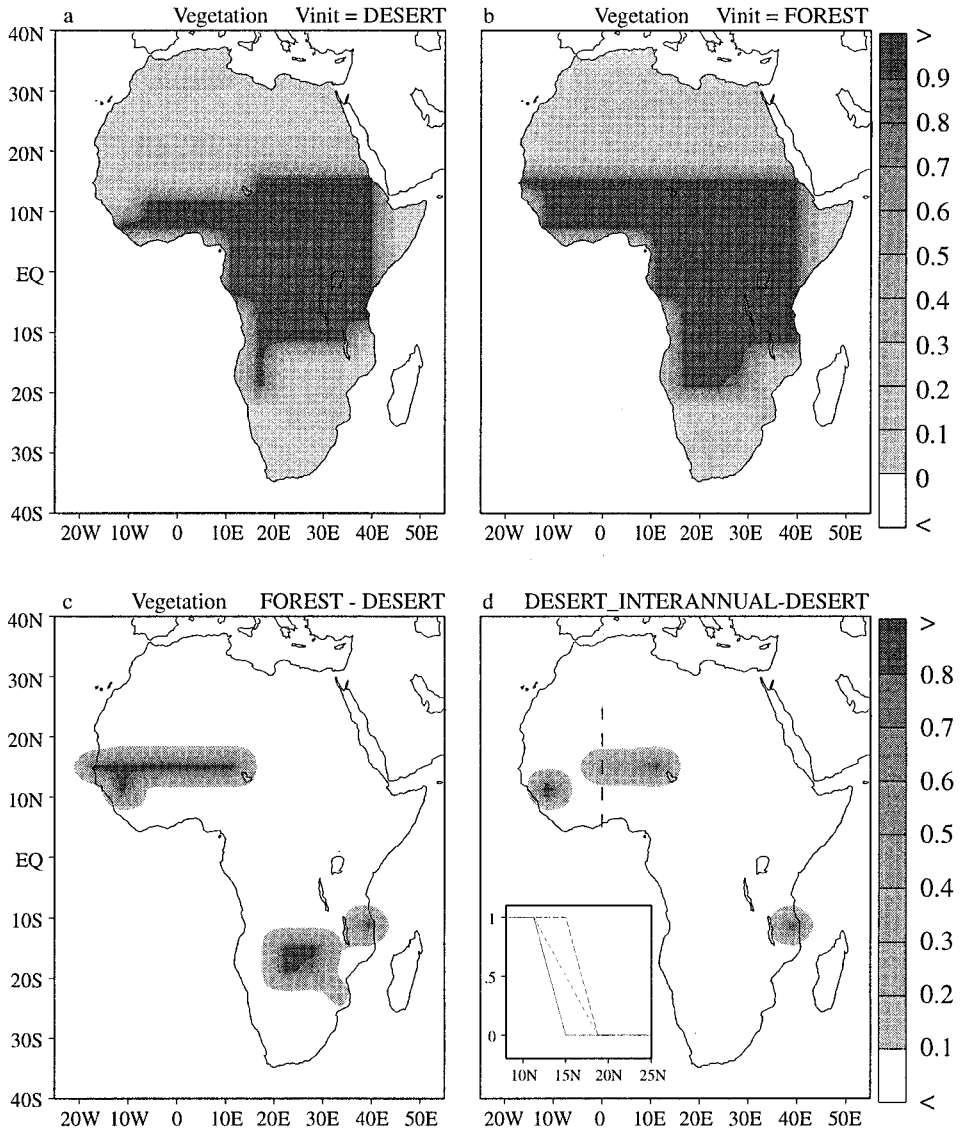

FIG. 1. Equilibrium distribution of African vegetation in a coupled atmosphere–land–vegetation model: (a) final vegetation distribution with the model starting from an initial state of desert over all of Africa (the V_{init} = DESERT run) and driven by climatological SST, (b) as in (a) but with the model starting from an initial state of forest over all of Africa (the V_{init} = FOREST run), (c) the difference between (b) and (a), (d) the difference between a run with interannual SST-anomaly forcing starting from all-desert initial condition (DESERT_INTERANNUAL) and (a). The values are averaged over the last 30 yr of the runs. The difference between (a) and (b) shows the existence of multiple equilibrium states in the Sahel region and southern Africa. The interannually forced run has a final vegetation cover somewhere between the DESERT run and the FOREST run, indicated by the fact that (d) is between zero and the values in (c). The inset in (d) shows the vegetation along 0°E in West Africa (thin line) for the three runs: the DESERT run (solid line), the FOREST run (dashed line), and the DESERT_INTERANNUAL run (dashed–dotted line).

mostly by atmosphere–ocean dynamics, here the SST are treated as a forcing on interannual timescales and their effect on the vegetation–atmosphere interaction is considered. Figure 2 shows the observed global SST difference between the mean of 1972–73 and 1982–84, and the mean of 1950, 1952–54, and 1958 derived from Reynolds and Smith (1994). It shows a dipole pattern in the Atlantic, with opposite signs in the Northern and Southern Hemispheres, and a signature of the El Niño–Southern Oscillation in the Pacific. The years are chosen after Folland et al. (1986) and correspond to wet or dry summers in the Sahel. The global SST anomaly is allowed to vary sinusoidally with an adjustable amplitude and period such that the total SST is

$$\text{SST} = \text{SST}_0 + F \sin(2\pi t/T)\,\text{SST}_a(x, y), \qquad (4)$$

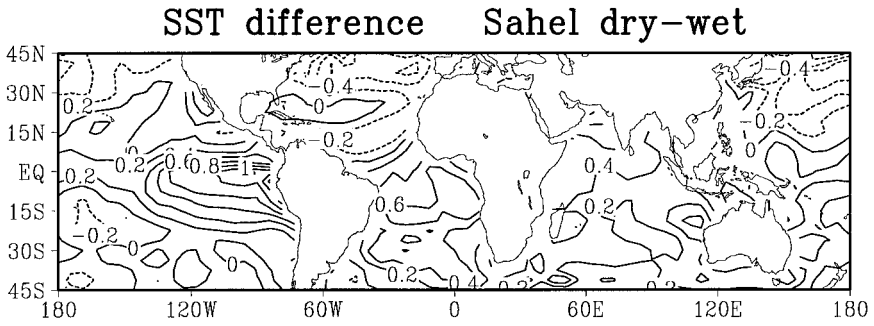

FIG. 2. Observed SST differences (the mean of 1972–73 and 1982–84 minus the mean of 1950, 1952–54, and 1958). This pattern is used to force the INTERANNUAL runs according to (4).

where SST_0 is the climatological SST, SST_a is the pattern shown in Fig. 2, x is longitude, y is latitude, t is time, F is the amplitude, and T is the forcing period. This total SST is used to force the coupled vegetation–land–atmosphere model.

Two experiments are conducted using the final vegetation distribution as the initial conditions from the DESERT run (called ''DESERT_INTERANNUAL'') and the FOREST run (''FOREST_INTERANNUAL''), respectively. In these experiments, F is set to 2. Although the response to interannual and decadal forcing can be quantitatively different for different forcing frequencies, the regime transition behavior is similar. Here one case with T taken as 6 yr is presented. Figure 1d shows the difference between the DESERT_INTERANNUAL run and the DESERT run, averaged over the last 30 yr of the 250-yr runs. Comparison with Fig. 1c indicates that the interannually forced run settles at a state in between the DESERT run and the FOREST run for the model ''Sahel'' region, as indicated by the fact that the values are between zero and those of Fig. 1c. This state may be termed ''grasslike'' and happens despite the steep vegetation response to precipitation [(3)] that leads to either a desertlike state or a forestlike state in the absence of the interannual SST forcing. A meridional cross section along the Greenwich meridian in the inset in Fig. 1d shows the more gradual transition in the INTERANNUAL case in comparison with the DESERT or the FOREST case (note the model's coarse resolution).

To see how this behavior evolves in time, Fig. 3 shows the vegetation averaged over the model Sahel region (10°–20°N, 15°W–20°E). The DESERT and FOREST runs approach their respective equilibrium vegetation of 0.31 and 0.71. The forced runs reach normalized vegetation values of 0.5 and 0.53, respectively, and are still approaching each other at the end of the run. The vegetation (thin lines) is nonsteady and oscillates with a period of 6 yr in response to the SST anomaly forcing but with a small amplitude, and the precipitation also oscillates but with a much larger amplitude (not shown), because the vegetation responds in a delayed and damped fashion because of its longer timescale. The precipitation (result of changes in the atmospheric circulation) acts as the link to pass the SST information to vegetation, which, in turn, feeds back on the precipitation.

To view this surprising regime transition in the final equilibrium states better, five more pairs of experiments similar to the INTERANNUAL runs but with F taken as 0.5, 1, 1.5, 2, 2.5 (the $F = 2$ pair is identical to INTERANNUAL) are presented. Figure 4 shows Sahel vegetation (same quantity as in Fig. 3) averaged over last 30

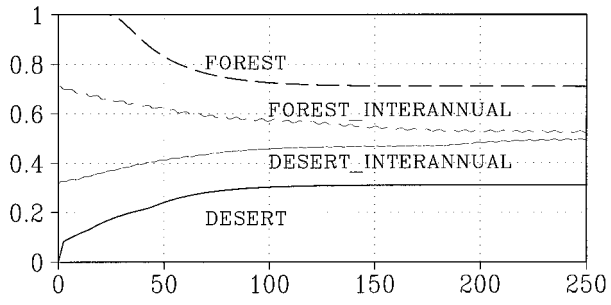

FIG. 3. Average vegetation over the model Sahel region (10°–20°N, 15°W–20°E) as a function of time (in years) in the runs: DESERT (thick solid line), FOREST (thick dashed line), DESERT_INTERANNUAL (thin solid line), FOREST_INTERANNUAL (like DESERT_INTERANNUAL, with the final state of the FOREST run as initial condition; thin dashed line). The first three runs correspond to Fig. 1. The vegetation slowly approaches an intermediate grasslike state in the INTERANNUAL runs.

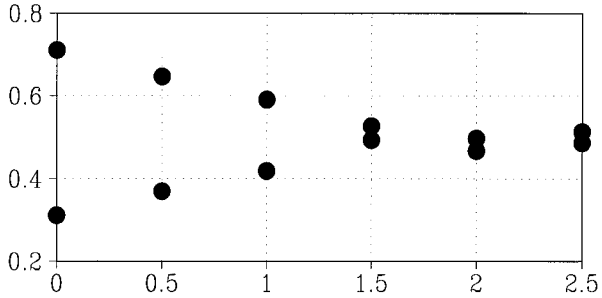

FIG. 4. Sahel vegetation averaged over the last 30 yr of the runs as a function of the amplitude F of the interannual SST variability [(4)]. The runs on the lower branch started from an all-desert condition, and the runs on the upper branch started from an all-forest condition. The two branches converge toward an intermediate grasslike state as the SST variability increases. The transition occurs at approximately $F = 1.5$.

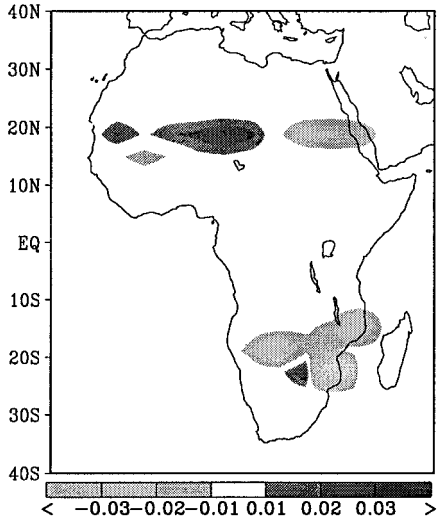

FIG. 5. Difference in normalized vegetation between a run forced by climatological SST and a run forced by repeating observed SST from 1950 to 1998. Results are averaged over the last 49 yr of the 250-yr runs.

yr of these 250-yr runs as a function of F. At weak forcing, two branches exist that correspond to the desertlike and the forestlike final states. As F increases, the two branches approach each other toward an intermediate grasslike state. Precipitation over these regions has a similar trend. The transition from multiple equilibria to a single equilibrium occurs at about $F = 1.5$, which corresponds to a forcing somewhat larger than the observed decadal SST variation amplitude ($F \approx 1$).

The parameter value used to obtain multiple equilibria ($a = 64$) corresponds to a very strong vegetation response to rainfall change near the inflection point P_0. Two model runs with more realistic value of $a = 4$ also were conducted. One run was forced by climatological SST, and the other was forced by observed SST from 1950 to 1998. The 49-yr-observed SST record was repeated several times for the 250-yr model run. Figure 5 shows the difference between these two runs for vegetation distribution averaged over the last 49 yr of the runs.

The largest differences occur again around the desert–forest boundary regions in the Sahel and southern Africa. The climatological vegetation and rainfall patterns (not shown) are similar to the $a = 64$ cases but with a smoother transition between desert and forest. The precipitation variability from varying SST enhances vegetation in the originally drier zones to the north in the Sahel and to the south in southern Africa, and the adjacent zones equatorward show the opposite tendency. As a result, the desert–forest transition is smoother in the varying-SST run than in the climatological-SST run. The magnitude of the differences is relatively small (typically about 0.03 in V, although one region in southern Africa has a value larger than 0.2). This effect is less dramatic than in the case with multiple equilibria (Figs. 3 and 4).

4. Conclusions

The nonlinearities in the coupled vegetation–climate system, including, in particular, the saturation behavior of the vegetation response [(3)] at low- and high-precipitation values, are responsible for the smoothing of gradient and the transition toward an intermediate state. Because of the nonlinearities, the system response can be stronger at the positive phase than at the negative phase of the sinusoidal forcing, so a net gain is accumulated over a full forcing cycle.

The shaping of a natural savanna ecosystem is related closely to climate variability and disturbances (Ellis and Swift 1988; Schimel et al. 1997). The modeling results presented here suggest that vegetation plays an active role in this interaction. Without external climate variability, the positive feedbacks from vegetation tend to enhance desert and forest regions at the expense of the savanna. Through nonlinearities in the coupled system, the interannual climate variability (in this case from SST variability) tends to smooth out the otherwise strong transition between forest and desert, thus contributing to the maintenance of a nonsteady, grasslike state.

Acknowledgments. We have benefited from discussions with P. Cox, R. Iacono, A. Mariotti, and A. Sutera. The authors also thank K. Hales and J. Meyerson for their graphical assistance. This research was supported by NSF Grant ATM-9521389, NOAA Grant NA86GP0314, and a grant to NZ from ICTP/ENEA, Italy.

REFERENCES

Bonan, G. B., D. Pollard, and S. L. Thompson, 1992: Effects of boreal forest vegetation on global climate. *Nature,* **359,** 716–718.

Brovkin, V., M. Claussen, V. Petouknov, and A. Ganopolski, 1998: On the stability of the atmosphere–vegetation system in the Sahara/Sahel region. *J. Geophys. Res.,* **103,** 31 613–31 624.

Charney, J. G., 1975: Dynamics of deserts and droughts in Sahel. *Quart. J. Roy. Meteor. Soc.,* **101,** 193–202.

Claussen, M., 1994: On coupling global biome models with climate models. *Climate Res.,* **4,** 203–221.

——, 1998: On multiple solutions of the atmosphere–vegetation system in present-day climate. *Global Biogeochem. Cycles,* **4,** 549–559.

——, and Coauthors, 1998: Modelling global terrestrial vegetation–climate interaction. *Philos. Trans. Roy. Soc. London,* **353B,** 53–63.

Dickinson, R. E., and A. Henderson-Sellers, 1988: Modeling tropical deforestation: A study of GCM land-surface parameterizations. *Quart. J. Roy. Meteor. Soc.,* **114,** 439–462.

——, M. Shaikh, R. Bryant, and L. Graumlich, 1998: Interactive canopies for a climate model. *J. Climate,* **11,** 2823–2836.

Ellis, J. E., and D. M. Swift, 1988: Stability of African pastoral ecosystems: Alternate paradigms and implications for development. *J. Range Manage.,* **41,** 450–459.

Foley, J. A., and Coauthors, 1996: An integrated biosphere model of land surface processes, terrestrial carbon balance, and vegetation dynamics. *Global Biogeochem. Cycles,* **10,** 603–628.

——, and Coauthors, 1998: Coupling dynamic models of climate and vegetation. *Global Change Biol.,* **4,** 561–579.

Folland, C. K., T. N. Palmer, and D. E. Parker, 1986: Sahel rainfall and worldwide sea temperatures, 1901–85. *Nature,* **320,** 602–607.

Ganopolski, A., and Coauthors, 1998: The influence of vegetation–

atmosphere–ocean interaction on climate during the mid-Holocene. *Science,* **280,** 1916–1919.

Goward, S. N., and S. D. Prince, 1995: Transient effects of climate on vegetation dynamics—satellite observations. *J. Biogeogr.,* **22,** 549–564.

Henderson-Sellers, A., 1993: Continental vegetation as a dynamic component of a global climate model: A preliminary assessment. *Climatic Change,* **23,** 337–378.

Ji, J.-J., 1995: A climate–vegetation interaction model: Simulating physical and biological processes at the surface. *J. Biogeogr.,* **22,** 445–451.

Lean, J., and D. A. Warrilow, 1989: Simulation of the regional climatic impact of Amazon deforestation. *Nature,* **342,** 411–413.

Lieth, H., 1975: Modeling the primary productivity of the world. *Primary Productivity of the Biosphere,* H. Leith and R. H. Whittaker, Eds., Springer-Verlag, 237–263.

Neelin, J. D., and N. Zeng, 2000: A quasi-equilibrium tropical circulation model—formulation. *J. Atmos. Sci.,* **57,** 1741–1766.

Nicholson, S. E., C. J. Tucker, and M. B. Ba, 1998: Desertification, drought, and surface vegetation: An example from the West African Sahel. *Bull. Amer. Meteor. Soc.,* **79,** 815–829.

Prentice, I. C., W. Cramer, S. P. Harrison, R. Leemans, R. A. Monserud, and A. M. Solomon, 1992: A global biome model based on plant physiology and dominance, soil properties and climate. *J. Biogeogr.,* **19,** 117–134.

Reynolds, R. W., and T. M. Smith, 1994: Improved global sea surface temperature analyses using optimum interpolation. *J. Climate,* **7,** 929–948.

Schimel, D. S., VEMAP participants, and B. H. Braswell, 1997: Continental scale variability in ecosystem processes: Models, data, and the role of disturbance. *Ecol. Monogr.,* **67,** 251–271.

Sellers, P. J., and Coauthors, 1996: A revised land surface parameterization (SiB2) for atmospheric GCMs. Part I: Model formulation. *J. Climate,* **9,** 676–705.

Shukla, J., C. Nobre, and P. Sellers, 1990: Amazon deforestation and climate change. *Science,* **247,** 1322–1325.

Sud, Y. C., G. K. Walker, J.-H. Kim, G. E. Liston, P. J. Sellers, and W. K.-M. Lau, 1996: Biogeophysical consequences of a tropical deforestation scenario: A GCM simulation study. *J. Climate,* **9,** 3225–3247.

Wang, G., and E. A. B. Eltahir, 2000: Biosphere–atmosphere interactions over West Africa. 2. Multiple climate equilibria. *Quart. J. Roy. Meteor. Soc.,* in press.

Woodward, F. I., 1987: *Climate and Plant Distribution.* Cambridge University Press, 174 pp.

Xue, Y., and J. Shukla, 1993: The influence of land surface properties on Sahel climate. Part I: Desertification. *J. Climate,* **6,** 2232–2245.

Zeng, N., J. D. Neelin, W. K.-M. Lau, and C. J. Tucker, 1999: Enhancement of interdecadal climate variability in the Sahel by vegetation interaction. *Science,* **286,** 1537–1540.

——, ——, and C. Chou, 2000: A quasi-equilibrium tropical circulation model—implementation and simulation. *J. Atmos. Sci.,* **57,** 1767–1796.

Zhang, H., A. Henderson-Sellers, and K. McGuffie, 1996: Impacts of tropical deforestation. Part I: Process analysis of local climatic change. *J. Climate,* **9,** 1497–1517.